

Quantum Imaging and Selection Rules in Triangular Quantum Corrals

Nikolaos A. Stavropoulos and Dirk K. Morr

Department of Physics, University of Illinois at Chicago, Chicago, IL 60607

(Dated: November 15, 2018)

We study quantum imaging in a triangular quantum corral that is embedded in a superconducting host system with s -wave symmetry. We show that the corral acts as a *quantum copying machine* by creating multiple images of a *quantum candle*. We obtain new selection rules for the formation of quantum images that arise from the interplay of the corral's geometry and the location of quantum candles. In more complex corral structures, we show that quantum images can be projected "around the corner".

PACS numbers: 73.22.-f, 73.22.Gk, 72.10.Fk, 74.25.Jb

Over the last few years, a growing number of exciting quantum phenomena has been observed [1, 2, 3, 4, 5] that arise from the interplay between the geometry and quantum properties of nanoscale atomic structures and their coupling to a fermionic quantum many-body systems. Among these phenomena are the formation of *quantum images* (also referred to as *quantum mirages*) in elliptical quantum corrals [1], electronic lifetime effects in triangular quantum corrals [3], and magnetization effects in triangular Co islands [4]. While the investigation of these phenomena is of general fundamental interest, it could potentially lead to important applications in the field of spin electronics and quantum information technology [6]. Theoretically, much progress in understanding the interaction between nanostructures and quantum many-body systems has been made by studying the formation of a *single* quantum image in quantum corrals that are embedded in metallic [7, 8] or superconducting (SC) [9] host systems.

In this Letter, we argue that complex nanoscale structures are prototype systems for the observation of novel quantum phenomena. In particular, we demonstrate that a triangular quantum corral can be used as a *quantum copying machine* that creates multiple quantum images of characteristic features (so-called *quantum candles*) in the host system's density-of-states (DOS). As a quantum candle, we employ the spectroscopic signature of a fermionic bound state induced by a magnetic impurity in a superconducting host system with s -wave symmetry. We show that the formation of quantum images inside a triangular corral consisting of *non-magnetic* impurities is determined by a set of selection rules that arises from the interplay between the corral's geometry and the location of quantum candles. Moreover, we demonstrate that such a corral can suppress the formation of fermionic bound states, leading to the important result that *non-magnetic impurities* can reverse the pair-breaking effect of a *magnetic defect*. Finally, we show that *double triangular corrals* allow the projection of quantum images "around the corner", opening the interesting possibility to custom design the imaging properties of quantum corrals.

In order to study novel quantum effects arising from

the interaction of a triangular quantum corral with a superconducting host system, we employ a generalized scattering \hat{T} -matrix theory [9, 10, 11]. The host system's local Greens function (in Nambu-notation) in the presence of the corral is given by

$$\hat{G}(\mathbf{r}, \mathbf{r}', \omega_n) = \hat{G}_0(\mathbf{r}, \mathbf{r}', \omega_n) + \sum_{i,j=1}^N \hat{G}_0(\mathbf{r}, \mathbf{r}_i, \omega_n) \hat{T}(\mathbf{r}_i, \mathbf{r}_j, \omega_n) \hat{G}_0(\mathbf{r}_j, \mathbf{r}', \omega_n), \quad (1)$$

where the sum runs over the locations \mathbf{r}_i ($i = 1, \dots, N$) of the N impurities forming the corral. The \hat{T} -matrix follows from the Bethe-Salpeter equation

$$\hat{T}(\mathbf{r}_i, \mathbf{r}_j, \omega_n) = \hat{V}_i \delta_{i,j} + \hat{V}_i \sum_{l=1}^N \hat{G}_0(\mathbf{r}_i, \mathbf{r}_l, \omega_n) \hat{T}(\mathbf{r}_l, \mathbf{r}_j, \omega_n); \quad (2)$$

$$\hat{V}_i = \frac{1}{2} (U_i \sigma_0 + J_i S \sigma_3) \tau_3, \quad (3)$$

and the electronic Greens function of the unperturbed (clean) system in momentum space is

$$\hat{G}_0^{-1}(\mathbf{k}, i\omega_n) = [i\omega_n \tau_0 - \epsilon_{\mathbf{k}} \tau_3] \sigma_0 + \Delta_0 \tau_2 \sigma_2. \quad (4)$$

$U_i (J_i)$ is the potential (magnetic) scattering strength of the impurity at site \mathbf{r}_i , S is the spin of a magnetic impurity, and σ , τ are the Pauli-matrices in spin and Nambu space, respectively. Δ_0 is the superconducting s -wave gap, and $\epsilon_{\mathbf{k}}$ is the host system's normal state dispersion. In this approach, magnetic impurities are treated as classical variables [11] (corresponding to a large- S limit) since J is taken to be smaller than the critical value J_c necessary for a Kondo-effect to occur in an s -wave superconductor [12], in full agreement with experiment [13]. Finally, the local DOS, $N(\mathbf{r}, \omega)$, shown below, is obtained numerically from Eqs.(1)-(4) with $N(\mathbf{r}, \omega) = A_{11} + A_{22}$, $A_{ii}(\mathbf{r}, \omega) = -\text{Im} \hat{G}_{ii}(\mathbf{r}, \omega + i\delta)/\pi$ and $\delta = 0.1$ meV.

Motivated by recent experiments [3], we first study the eigenmode spectrum of a triangular equilateral quantum corral embedded in a normal host system. To facilitate comparison with experiment, we consider a two-dimensional host system with a triangular lattice (lattice

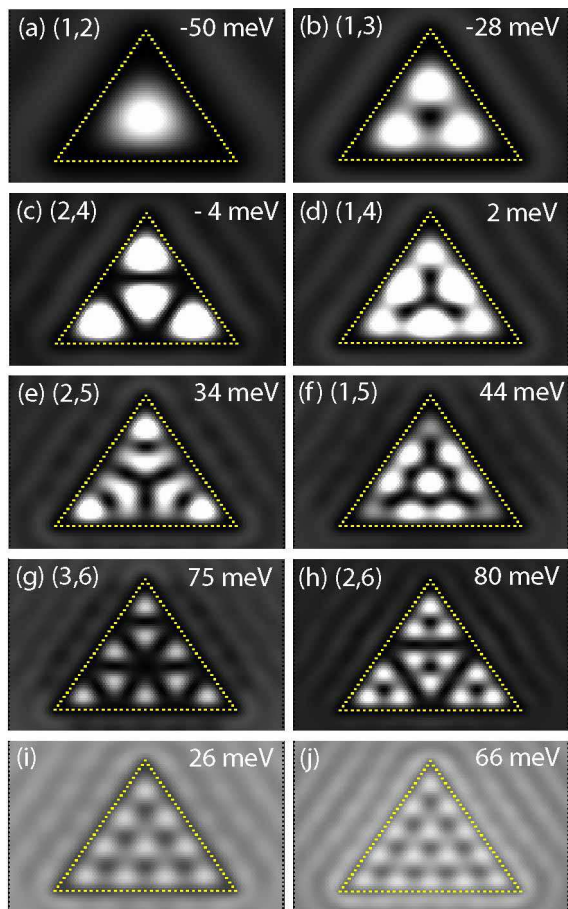


FIG. 1: (a)-(h) Spatial DOS plot for the eight lowest energy eigenmodes (eigenmode energy is shown in the upper right corner) in the unitary scattering limit ($U_i = 4$ eV). (m,l) are the quantum numbers of the corresponding TPW eigenstate. (i),(j) Eigenmodes of the corral for $U_i = 0.5$ eV.

constant $a_0 = 1$) and $\epsilon_{\mathbf{k}} = k^2/2m - \mu$ ($\hbar = 1$) where $\mu = -65$ meV is the chemical potential and $k_F = 0.24$ the Fermi wave-vector (qualitatively similar results to the ones shown below are expected for a 3D host system). In Fig. 1(a)-(h) we present a spatial DOS plot of the eight lowest energy eigenmodes [with light (dark) regions indicating a large (small) DOS] for a corral consisting of 90 *non-magnetic* impurities with $U_i = 4$ eV (the impurities are represented by filled yellow squares, separated by $\Delta r = 2$). In this unitary scattering limit, the eigenmodes (i.e., their spatial structure and ordering in energy) are well described by the eigenstates, ϕ_{lm} , of an infinitely deep triangular potential well (TPW) [14] [the corresponding quantum numbers (m,l) are shown in the upper left corner of Figs. 1(a)-(h)]. With decreasing U_i , the energy separation of the eigenmodes is reduced. In addition, new eigenmodes emerge, such as the ones shown in Figs. 1(i),(j) for $U_i = 0.5$ eV, which are similar to those observed experimentally (cf. Fig.1(d) in Ref. [3]).

The spatial form of the corral's eigenmodes opens the

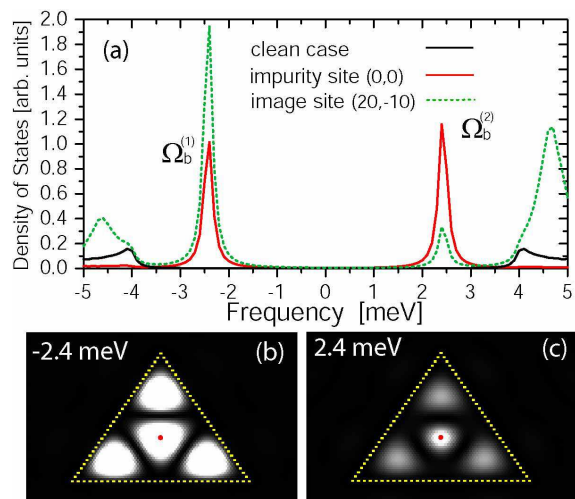


FIG. 2: (a) DOS as a function of frequency. (b),(c) Spatial DOS plot at the bound state energies $\Omega_b^{(1,2)} = \mp 2.4$ meV.

possibility to form multiple *quantum mirages*. To demonstrate the qualitative nature of this effect, we retain the above parameters and take the superconducting gap to be $\Delta_0 = 4$ meV, yielding a superconducting coherence length $\xi_c = k_F/(m\Delta_0) = 135$. As the quantum candle whose image is formed we use the spectroscopic signature of a fermionic bound state induced by a single magnetic impurity ($J_i = 1.0$ eV), located in the center of the corral at $\mathbf{r}_1 = (0,0)$. This signature consists of a particlelike and holelike peak in the DOS at energies $\Omega_b^{(1,2)} = \mp 2.4$ meV, as shown in Fig. 2a. In Figs. 2(b),(c) we present spatial DOS plots at $\Omega_b^{(1,2)}$ (the location of the magnetic impurity is shown as a filled red circle). The formation of the impurity bound state is accompanied by the excitation of the (2,4)-eigenmode [Fig. 1(c)] and by the emergence of three images of the bound state peaks inside the corral. Note that only eigenmodes that possess sufficiently large spectral weight at the impurity site and are close in energy to $\Omega_b^{(1,2)}$ are relevant for the formation of quantum images. Since the energy of the (2,4)-eigenmode, $E_{(2,4)} = -4$ meV, is closer to $\Omega_b^{(1)}$ than to $\Omega_b^{(2)}$, the spectral weight of the quantum images is larger at $\Omega_b^{(1)}$ than at $\Omega_b^{(2)}$. This result demonstrates that a triangular quantum corral acts as a *quantum copying machine* for distinct features in the DOS. Moreover, the corral's imaging properties can be specifically designed since changing the corral's size leads to a shift in the eigenmode energies [14]. For example, in a corral consisting of 117 impurities, the imaging properties in the SC state are determined by the (1,5)-mode [$E_{(1,5)} = 0$ meV] leading to a different spatial pattern of the quantum images [15]. Finally, we note as an important result that the formation of an impurity bound state can be completely suppressed inside the corral. To demonstrate

this effect, we place the magnetic impurity at a node $[\mathbf{r}_1 = (-5, -5)]$ of the (2, 4)- and (1, 4)-eigenmodes, as shown in Fig. 3(a) for $|\omega| > \Delta_0$. In this case, the DOS at \mathbf{r}_1 [Fig. 3(b)] does not possess any signature of an induced bound state and hence, no image is observed anywhere inside the corral. This complete suppression arises from the incompatibility of the bound state with the boundary conditions provided by the corral's wall. In other words, an impurity bound state can only be formed if it can couple to one of the corral's eigenmodes. The importance of this result lies in the fact that while non-magnetic impurities cannot induce a fermionic bound state in an *s*-wave superconductor, they can suppress its formation and thus reverse the pair-breaking effect of a *magnetic defect*.

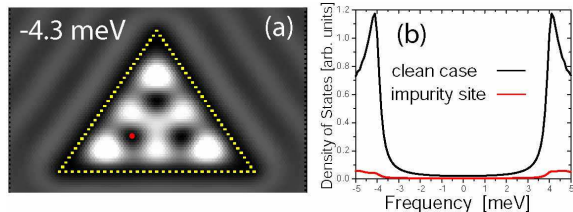


FIG. 3: (a) Spatial DOS plot for $|\omega| > \Delta_0$. (b) DOS at the site of the magnetic impurity.

Next, we consider the effects of two magnetic impurities located inside the corral at $\mathbf{r}_1 = (-10, -10)$ and $\mathbf{r}_2 = (20, -10)$. The angle, α , between the impurity spins is determined by the interaction between them. In what follows, we assume a ferromagnetic alignment of the spins ($\alpha = 0$), however, results similar to those shown below are also obtained for $\alpha \neq 0$. Quantum interference of scattered electronic waves leads to the formation of even and odd impurity bound states (with respect to a vertical axis midway between the two impurities) and a splitting of the bound state energies [16]. As a result, the DOS exhibits four peaks at $\Omega_o^{(1,2)} = \mp 2.8$ meV and $\Omega_e^{(1,2)} = \mp 2.0$ meV [see Fig. 4(a)]. The formation of quantum images requires that the even/odd bound states couple to corral eigenmodes of the same symmetry. The eigenstates of a TPW and thus the corral eigenmodes transform under reflection at the vertical axis as $\phi_{lm} \rightarrow -\exp[i2\pi(m+l)/3]\phi_{lm}^*$ [14]. While ϕ_{24} is imaginary and thus even under reflection, an even and odd wave-function is formed from ϕ_{14} via $\phi_{14}^{(e,o)}(x) = \phi_{14}(x) \pm \phi_{14}(-x)$. In Figs. 4(b),(e) we plot the DOS at $\Omega_o^{(1,2)}$ whose spatial form agrees well with that of $|\phi_{14}^{(o)}|^2$ shown in the inset of Fig. 4(a). We therefore conclude that $\Omega_o^{(1,2)}$ are the frequencies of the odd bound state, while $\Omega_e^{(1,2)}$ are the energies of the even bound state whose spatial DOS is shown in Figs. 4(c),(d). The imaging properties of the corral are thus frequency dependent due to the interplay between the corral's geometry and the location of the quantum candles.

This interplay can be further studied by placing three

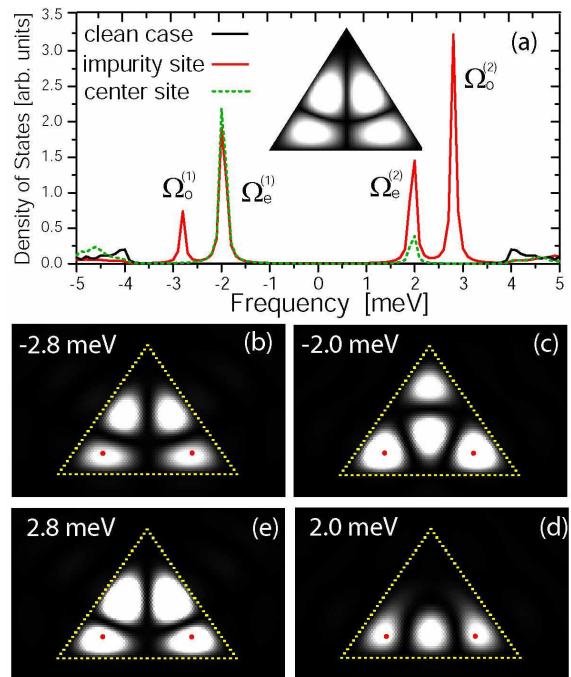


FIG. 4: (a) DOS as a function of frequency. Inset: Spatial plot of $|\phi_{14}^{(o)}|^2$. (b)-(e) Spatial DOS plot for the odd [(b) and (e)] and even [(c) and (d)] impurity bound states.

magnetic impurities with parallel spins at the corners of an equilateral triangle at $\mathbf{r}_1 = (-10, -10)$, $\mathbf{r}_2 = (20, -10)$, and $\mathbf{r}_3 = (-10, 20)$. Since the degeneracy of the impurity bound states is again lifted via quantum interference, we expect to find six peaks in the DOS. Instead, the DOS exhibits four peaks, as shown in Fig. 5(a), corresponding to the presence of only two non-degenerate impurity states. This reduction to two impurity states arises from a new type of selection rule that is based on the interplay between the corral geometry and the location of the quantum candles. Under a rotation of $2\pi/3$ around the corral's center, ϕ_{lm} , and hence the corral eigenmodes, transform as $\phi_{lm} \rightarrow \exp[i2\pi(m+l)/3]\phi_{lm}$. Due to their geometry the non-degenerate impurity bound states possess the same transformation properties, and their formation thus requires that they couple to eigenmodes with $n = (m+l) \bmod 3 = 1, 2, 3$. However, the eigenmodes with $n = 1$ are at energies $|E_{(m,l)}| \gg \Delta_0$, thus preventing the creation of the bound state with $n = 1$. As a result, only the bound states with $n = 0$ [Figs. 5(c) and (d)] and $n = 2$ [Figs. 5(b) and (e)] are formed via their coupling to the (2, 4)- [Fig. 1(c)] and (1, 4)-eigenmodes [Fig. 1(d)], respectively.

More complex corral structures can be employed to project quantum images "around the corner". To demonstrate this effect, we insert a triangular corral with 42 *non-magnetic* impurities ($U_i = 4$ eV) into the corral discussed above. In the normal state, two eigenmodes of

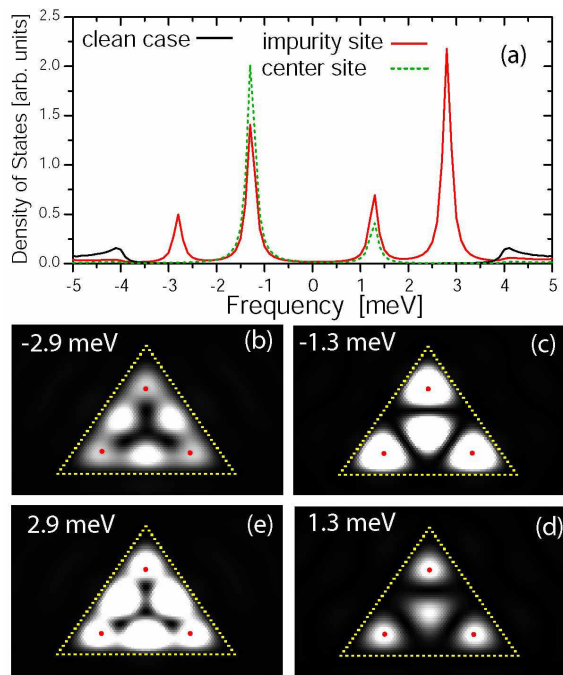


FIG. 5: (a) DOS as a function of frequency. (b)-(d) Spatial plot of the DOS for the impurity bound state with $n = 2$ [(b) and (e)] and $n = 0$ [(c) and (d)].

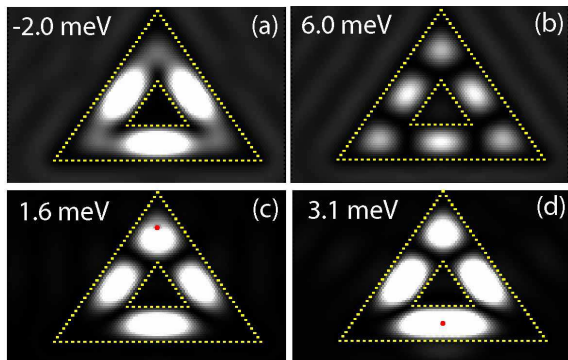


FIG. 6: Normal state eigenmodes of a double triangular quantum corral. (c),(d) Spatial DOS plot for two different locations of a magnetic impurity with (c) $\Omega_b^{(2)} = 1.6$ meV and (d) $\Omega_b^{(2)} = 3.1$ meV.

this double corral [Figs. 6(a) and (b)] possess energies that render them relevant for the formation of quantum images. By placing a magnetic impurity ($J_i = 2$ eV) between the apices of the triangles in the SC state [Fig. 6(c)] a quantum image is formed “around the corner” between the triangles’ bases. Similarly, a quantum image is created between the apices by placing the magnetic impurity between the triangles’ bases [Fig. 6(d)]. Note the significant shift in Ω_b when the position of the impurity is changed. This result opens the interesting possibility to custom design the imaging properties of quantum corrals

to form mirages at arbitrary locations.

Finally, we note that the qualitative features of our results presented above are robust against changes in the band parameters or Δ_0 , as long as ξ_c is larger than the size of the corral. Moreover, whether a Kondo-effect can occur inside a corral and how it is affected by the corral’s eigenmodes is an interesting but non-trivial question whose study we reserve for future work [15].

In summary, we demonstrate that the eigenmode spectrum of a triangular quantum corral can be employed (i) to create multiple images of a quantum candle, and (ii) to suppress the formation of impurity bound states. We obtain new selection rules for quantum imaging that arise from the interplay of the corral’s geometry and the location of quantum candles. Finally, we show that more complex nanostructures allow the projection of quantum images “around the corner”.

We would like to thank K.-F. Braun, J.C. Davis, O. Pietzsch, and R. Wiesendanger for stimulating discussions, and would especially like to thank K.-H. Rieder for a series of discussions that motivated this work. D.K.M. acknowledges financial support from the Alexander von Humboldt foundation.

-
- [1] H.C. Manoharan, C.P. Lutz, and D.M. Eigler, *Nature (London)* **403**, 512 (2000).
 - [2] A.W. Holleitner *et al.*, *Phys. Rev. Lett.* **87**, 256802 (2001); D.J. Derro *et al.*, *Phys. Rev. Lett.* **88**, 097002 (2002); C. Chicanne *et al.*, *Phys. Rev. Lett.* **88**, 097402 (2002).
 - [3] K.-F. Braun and K.-H. Rieder, *Phys. Rev. Lett.* **88**, 096801 (2002).
 - [4] O. Pietzsch *et al.*, *Phys. Rev. Lett.* **92**, 057202 (2004).
 - [5] J. Repp *et al.*, *Phys. Rev. Lett.* **92**, 036803 (2004).
 - [6] S.A. Wolf *et al.*, *Science* **294**, 1488 (2001); B.E. Kane, *Nature (London)* **393**, 133 (1998).
 - [7] G.A. Fiete *et al.*, *Phys. Rev. Lett.* **86**, 2392 (2001); A.A. Aligia, *Phys. Rev. B* **64**, 121102 (2001); K. Hallberg, A.A. Correa, and C.A. Balseiro, *Phys. Rev. Lett.* **88**, 066802 (2002); D. Porrás *et al.*, *Phys. Rev. B* **63**, 155406 (2001); O. Agam and A. Schiller, *Phys. Rev. Lett.* **86**, 484 (2001); Y. Shimada *et al.*, *Surf. Sci* **514**, 89 (2002); M. Weissmann and H. Bonadeo, *Physica E* **10**, 544 (2001); M. Schmid and A.P. Kampf, *Ann. Phys.* **12**, 463 (2003).
 - [8] For a general review see G.A. Fiete and E.J. Heller, *Rev. Mod. Phys.* **75** 933 (2003), and references therein.
 - [9] D. K. Morr and N. A. Stavropoulos, *Phys. Rev. Lett.* **92**, 107006 (2004); *ibid.*, *Phys. Rev. B* **67**, 020502(R) (2003).
 - [10] D.K. Morr and A.V. Balatsky, *Phys. Rev. Lett.* **90**, 067005 (2003).
 - [11] Y. Lu, *Acta Physics Sinica* **21**, 75 (1965); H. Shiba, *Prog. Theoret. Phys.* **40**, 435 (1968).
 - [12] K. Satori *et al.*, *J. Phys. Soc. Jpn.* **61**, 3239 (1992).
 - [13] A. Yazdani *et al.*, *Science* **275**, 1767 (1997).
 - [14] H.R. Krishnamurthy *et al.*, *J. Phys. A: Math. Gen.* **15**, 2131 (1982).
 - [15] D.K. Morr and N.A. Stavropoulos, in preparation.
 - [16] No even/odd bound states are formed for $\alpha = \pi$ [9].